


EFFECTS OF GLASS FIBER SIZE AND CONTENT ON MICROSTRUCTURES AND PROPERTIES OF KNO_3 -BASED WATER-SOLUBLE SALT CORE FOR HIGH PRESSURE DIE CASTING

Xiaolong Gong, Wenming Jiang , Fuchu Liu, Zhiyuan Yang, Feng Guan, and Zitian Fan

State Key Laboratory of Materials Processing and Die and Mould Technology, Huazhong University of Science and Technology, Wuhan 430074, China

Copyright © 2020 American Foundry Society
<https://doi.org/10.1007/s40962-020-00480-9>

Abstract

The water-soluble salt core with higher bending strength and toughness is necessary to withstand the high pressure needed to manufacture some complex parts by high pressure die casting (HPDC). In this paper, the effects of glass fiber size and content on microstructures and properties of KNO_3 -based (KNO_3 -30 mol%KCl) water-soluble salt core were systematically studied. The results showed that increasing the glass fiber content greatly improved the bending strength and impact toughness of the KNO_3 -based salt core, decreased the water solubility rate and increased the humidity resistance. In addition, increasing the glass fiber size sharply enhanced the impact toughness of the KNO_3 -based salt core, while decreasing the bending strength, water solubility rate and humidity resistance. The maximum bending strength and impact toughness of the reinforced KNO_3 -based salt core with the glass fiber were, respectively, 41.32 ± 0.38 MPa and 2.146 ± 0.108 kJ/m²,

which were 55.9% and 315.1% higher than those of the unreinforced KNO_3 -based salt core, respectively. The microstructures show that the glass fibers were evenly distributed in the KNO_3 -based salt core, which significantly refined the KCl primary phases, especially for the 12.5- μm glass fiber. Meanwhile, many fiber pull-out holes were observed in the KNO_3 -based salt cores with 75- μm and 25- μm glass fiber. The grain refinement, fiber pull-out and crack deflection were the main mechanism for improving the strength and toughness of the KNO_3 -based salt core.

Keywords: salt core, potassium nitrate, glass fiber, water-soluble, high pressure die casting (HPDC), bending strength, impact toughness, microstructure characteristics

Introduction

Currently, the water-soluble salt core has attracted considerable attention in the manufacture of complex inner cavity and undercut structural parts due to its specific properties including excellent collapsibility, low gas evolution and high-dimensional accuracy.^{1,2} Inorganic salts, such as sodium chloride (NaCl), potassium chloride (KCl), sodium carbonate (Na_2CO_3) and sodium sulfate (Na_2SO_4), are widely used as the raw materials to fabricate the water-soluble salt core.³⁻⁶ Nevertheless, the inorganic salts are brittle materials and the unreinforced water-soluble salt core has poor mechanical properties.⁷ During high pressure die casting (HPDC), the water-soluble salt core is prone to brittle fracture.^{2,8-10} Furthermore, the salt core manufactured by casting methods is prone to occur the shrinkage on cooling and the high susceptibility to cracking, resulting in

a decrease in the strength of the salt core.^{2,7} Therefore, in order to meet the need of the die casting sector to look for higher strength cores to cast complex geometries through the HPDC process, the water-soluble salt core should be strengthened.

According to current research, the low-cost powder reinforcing materials, such as bauxite powder, mica powder and quartz powder, are commonly used to enhance the mechanical properties of the water-soluble salt core.^{7,11-14} Generally, the mechanical properties of the water-soluble multivariate salt core (prepared by two or more inorganic salts) are better than that of the water-soluble unary salt core, which is similar to the metal materials.^{3,15} Moreover, the microstructures of the water-soluble multivariate salt core mainly consist of a primary phase and a eutectic phase, and the powder reinforcing materials can refine the

microstructure of the water-soluble salt core, thereby improves the strength.^{16,17} However, the powder reinforcing materials cannot effectively enhance the impact resistance of the water-soluble salt core.⁷ In order to resist the impact of high-speed, high-pressure and high-density materials, the water-soluble salt core not only needs a high strength, but also needs a good impact toughness.^{18,19} Fiber materials are widely used in the strengthening of ceramic matrix composites due to their high tensile strength, good elastic coefficient and excellent thermal stability.²⁰⁻²² However, there are few reports on the strengthening of the water-soluble salt core by fiber materials. Whiskers have been investigated as a micron or a nanometer short fiber material to strengthen the salt core. Wan et al.²³ studied the strengthening of NaCl or KCl water-soluble salt core by aluminum borate whiskers, and the results indicate that the aluminum borate whiskers dramatically increased the bending strength of the salt core, but the study did not analyze the effect on impact toughness. Furthermore, as the content of the aluminum borate whisker increased, the agglomeration of the aluminum borate whisker was observed in the salt core. Therefore, the size and content of the fiber materials have a remarkable effect on the microstructures and mechanical properties of the water-soluble salt core.

In the present study, a commercial glass fiber with low price as a reinforcing material was used to strengthen the KNO₃-based (KNO₃-30 mol%KCl) water-soluble salt core for the high pressure die casting. The effects of glass fiber size and content on the bending strength, impact toughness, water solubility rate and hygroscopic rate of KNO₃-based water-soluble salt core were systematically investigated. Moreover, the microstructures of the KNO₃-based salt core strengthened by the glass fiber were studied, and the strengthening mechanism was also discussed. Finally, the KNO₃-based salt core with a complex shape was fabricated using the obtained optimal process.

Materials and methods

Raw materials

Potassium nitrate (KNO₃, 99% purity) and potassium chloride (KCl, 99% purity) were used as the matrix material in this study. Glass fibers with three sizes (Shenzhen Fiber Valley Technology Co., Ltd., China) were used as a reinforcing material, and their technical parameters and SEM morphologies are shown in Table 1 and Figure 1, respectively. Acetone (Analytical purity, Sinopharm Chemical Reagent Co., Ltd., China) as a solvent was used to clean the KNO₃-based salt core.

Table 1. Technical Parameters of Glass Fiber

Glass fiber sample	Average length (μm)	Diameter (μm)	Density (g/cm ³)	Loss on ignition (%)
1	74	9	2.4	< 0.5
2	25	9	2.4	< 0.5
3	12.5	9	2.4	< 0.5

Preparation process

Figure 2 shows a preparation process of the KNO₃-based salt core. The KNO₃, KCl and glass fiber were first mixed and dried, wherein the molar ratio of the KNO₃ and KCl was 70 mol%:30 mol%, and the glass fiber contents were 10 wt.%, 20 wt.% and 30 wt.%, respectively. The dried mixture (KNO₃, KCl and glass fiber) was then placed inside an iron crucible and melted using a resistance furnace at 495 °C. Subsequently, the molten salt was stirred 10 min using a metal stirrer. When the temperature of the molten salt was about 485 °C, the molten salt was quickly poured into a metal mold with a preheated temperature of 180 °C. Next, the metal mold was opened after cooling for 30 s, and the KNO₃-based salt core was taken out and cooled to room temperature. Finally, the KNO₃-based salt core was prepared. The salt core samples with two sizes were prepared by the above preparation process. The standard samples with 173 mm × 22.36 mm × 22.36 mm size were used to test the bending strength, and the samples with 80 mm × 10 mm × 10 mm size were used to test the impact toughness, water solubility rate and hygroscopic rate. The microstructure of the samples used to test the impact test toughness was also analyzed.

Characterization

The bending strength of the KNO₃-based salt core was measured using a three-point bending method on a SWY digital hydraulic strength testing machine. The impact toughness of the KNO₃-based salt core was measured using a simply supported beam impact tester with an impact speed of 2.9 m/s and a pendulum energy of 2.0 J. The water solubility rate of the KNO₃-based salt core was calculated according to Eqn. 1:

$$K = \frac{m}{s \times t} \quad \text{Eqn. 1}$$

where K represents the water solubility rate, m is the mass of the KNO₃-based salt core, s is the total surface area of the KNO₃-based salt core and t is the dissolution time of the KNO₃-based salt core in 80 °C water. The hygroscopic rate of the KNO₃-based salt core was calculated by Eqn. 2:

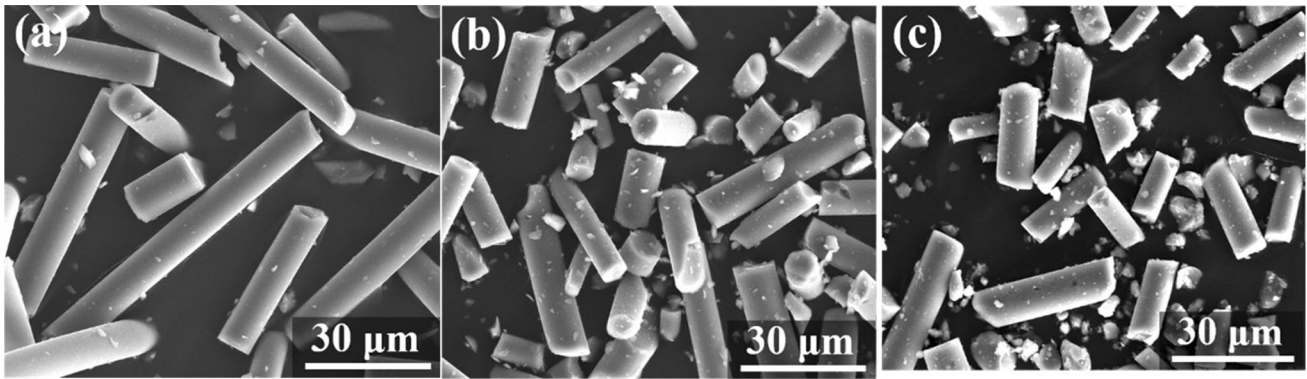


Figure 1. SEM morphologies of the glass fibers: (a) sample 1 (size = 74 μm), (b) sample 2 (size = 25 μm) and (c) sample 3 (size = 12.5 μm)

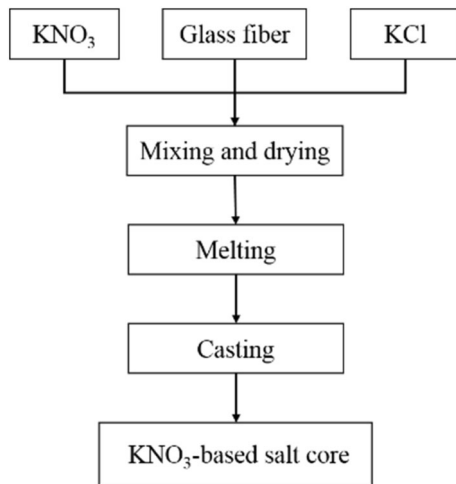


Figure 2. Preparation process of the KNO₃-based salt core

$$\psi = \frac{m_1 - m_0}{m_0} \times 100\% \quad \text{Eqn. 2}$$

where ψ represents the hygroscopic rate, m_0 is the original mass of the salt core samples and m_1 is the mass of the salt core sample exposed in air for 5 days.

A JD520 surface roughness tester was used to measure surface roughness of the KNO₃-based salt core. The microstructures of the KNO₃-based salt core samples and the glass fiber via previously treated with carbon sputtering were observed and analyzed using the Quanta 200 environmental scanning electron microscope (SEM) equipped with facilities for energy-dispersive spectrometer (EDS). The elemental compositions of the KNO₃-based salt core were detected via the EDS. The Image-Pro Plus software was used to measure the area of the KCl primary phase, and the measurement was taken on 50 different areas of each microstructure in order to minimize the errors. The

grain size of the KCl primary phase was calculated according to Eqn. 3:

$$D = 2\sqrt{A/\pi} \quad \text{Eqn. 3}$$

where D and A are, respectively, the grain size and area of the KCl primary phase.²⁴ All the test results were averaged over five measurements in order to minimize the error of the data.

Results and discussion

Effect of glass fiber on properties of the KNO₃-based salt core

Figure 3 exhibits the effect of glass fiber on bending strength and impact toughness of the KNO₃-based salt core. It can be seen from Figure 3a, b that the glass fiber has a remarkable effect on the bending strength and impact toughness of the KNO₃-based salt core. As the content of the glass fiber increases, the bending strength and impact toughness of the KNO₃-based salt core dramatically increase. With the further increase in the glass fiber content, the molten salt has insufficient fluidity, and the misrun defect occurred during the casting process, resulting in a large hole in the salt core sample, which seriously affects the performance of the salt core. Furthermore, the bending strength of the KNO₃-based salt core decreases with the increase in the glass fiber size. When the glass fiber (30 wt.%) size increases from 12.5 μm to 74 μm, the bending strength of the KNO₃-based salt core decreases from 41.32 ± 0.38 MPa to 38.85 ± 0.72 MPa. As can be seen from Figure 3b, increasing the size of glass fiber can increase the impact toughness of the KNO₃-based salt core. When the glass fiber (30 wt.%) size increases from 12.5 μm to 74 μm, the impact toughness of the KNO₃-based salt core greatly increases from 0.903 ± 0.003 kJ/m² to 2.146 ± 0.108 kJ/m². Therefore, in order to obtain a salt core with good comprehensive properties, the size and content of the glass fiber must be considered.

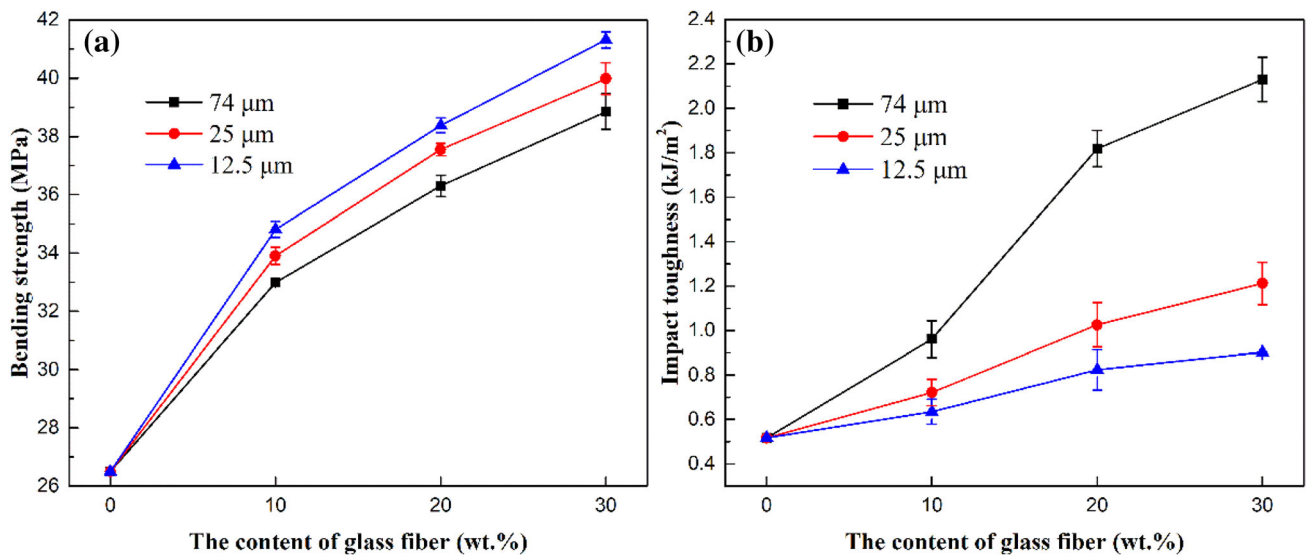


Figure 3. Effect of glass fiber on properties of the KNO₃-based salt core. (a) Bending strength; (b) impact toughness

Table 2 shows the water solubility rate and hygroscopic rate of the KNO₃-based salt core strengthened by the glass fiber. The water solubility and hygroscopic rate are also important performance parameters of the salt core, because the water solubility rate affects the removal rate of the core from the part and the hygroscopic rate affects the reduction in strength due to water absorption. As can be seen, the unreinforced KNO₃-based salt core has an excellent water solubility rate of $998.0 \pm 24.6 \text{ g}/(\text{min m}^2)$, and the hygroscopic rate is $0.281 \pm 0.02\%$. It should be noted that the glass fiber reduces the water solubility rate of the KNO₃-based salt core, but improves the humidity resistance. However, the size and content of the glass fiber have different effects on the water solubility rate and

hygroscopic rate of the salt core. For example, when the glass fiber size is 25 μm, the water solubility rate of the KNO₃-based salt core decreases from $673.8 \pm 20.7 \text{ g}/(\text{min m}^2)$ to $532.5 \pm 12.7 \text{ g}/(\text{min m}^2)$ with increasing the glass fiber content from 10 wt.% to 30 wt.%, and the hygroscopic rate shows the same trend decreasing from $0.156 \pm 0.019\%$ to $0.078 \pm 0.01\%$. When the glass fiber content is 30 wt.%, with the decrease in the glass fiber size from 74 μm to 12.5 μm, the water solubility rate of the KNO₃-based salt core increases from $472.4 \pm 6.8 \text{ g}/(\text{min m}^2)$ to $620.3 \pm 8.4 \text{ g}/(\text{min m}^2)$, while the hygroscopic rate shows the opposite trend decreasing from $0.080 \pm 0.01\%$ to $0.066 \pm 0.005\%$. Such phenomenon can be summarized by the fact that the higher the glass fiber content, the smaller the water solubility rate and hygroscopic rate of the salt core. Meanwhile, the larger glass fiber size, the lower water solubility rate and the greater hygroscopic rate of the salt core. This phenomenon is mainly attributed to two factors. On the one hand, the glass fiber as a water-insoluble material hinders the contact between water and the salt core, resulting in the water solubility rate and hygroscopic rate decrease. The more glass fiber content leads to a smaller contact area between water and the salt core. On the other hand, the smaller the glass fiber size, the easier it is to fall off during the dissolution of the salt core, and the less influence it has on the water solubility rate of the salt core.

Table 2. Water Solubility and Hygroscopic Rate of the KNO₃-Based Salt Core

Glass fiber		Water solubility rate (g/(min m ²))	Hygroscopic rate (%)
Size (μm)	Content (wt.%)		
–	0 (unreinforced)	998.0 ± 24.6	0.281 ± 0.02
74	10	621.1 ± 10.5	0.160 ± 0.015
	20	518.0 ± 11.3	0.145 ± 0.013
	30	472.4 ± 6.8	0.080 ± 0.01
25	10	673.8 ± 20.7	0.156 ± 0.019
	20	610.8 ± 4.5	0.131 ± 0.012
	30	532.5 ± 12.7	0.078 ± 0.01
12.5	10	769.8 ± 18.9	0.143 ± 0.015
	20	691.8 ± 14.7	0.118 ± 0.01
	30	620.3 ± 8.4	0.066 ± 0.005

Figure 4 presents the water-soluble experiments of the KNO₃-based salt core strengthened by 30 wt.% glass fiber with 25 μm size. It can be observed that the KNO₃-based salt core strengthened by the glass fiber can quickly dissolve in 80 °C water. It is well known that the solubility of the KNO₃ is 169 g in 100 g water (80 °C), and the glass fiber is a water-insoluble material.²⁵ As shown in Figure 4a–d, the water-insoluble glass fiber gradually falls off

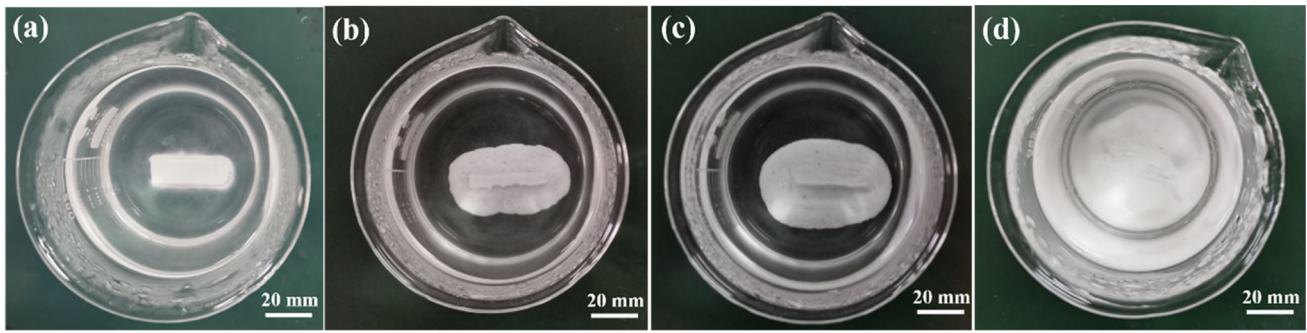


Figure 4. Water-soluble experiments of the KNO_3 -based salt core strengthened by 30 wt.% glass fiber (size = 25 μm) in 80 °C water: (a) 0 min; (b) 6 min; (c) 12 min; (d) 18 min

as the KNO_3 -based salt core sample is put into 80 °C water, and the KNO_3 -based salt core sample is completely dissolved after 18 min. It is noted that the excellent water solubility of the salt core can greatly improve the production efficiency of parts, especially for the complex inner cavity structural parts. Moreover, the glass fiber can be completely recycled and reused, reducing the manufacturing cost of the salt core.

Effect of glass fiber on microstructures of the KNO_3 -based salt core

Figure 5 reveals the fracture surface and EDS results of the KNO_3 -based salt core strengthened by 20 wt.% glass fiber with 25 μm size. It can be seen from the backscattered SEM image of Figure 5a that the glass fibers are evenly distributed in the KNO_3 -based salt core, and fiber pull-out holes (indicated in the yellow circles) are easily observed. According to the KNO_3 -KCl binary phase diagram,²⁶ the solidification microstructure of the KNO_3 -based salt core (KNO_3 -30 mol%KCl) is composed of KCl primary phase and $\text{KNO}_3 + \text{KCl}$ eutectic phase. As shown in Figure 5(a1–a3), the EDS results (corresponding to the red pane in Figure 5a) suggest that the microstructures of the KNO_3 -based salt core strengthened by glass fiber consist of KCl primary phase, $\text{KNO}_3 + \text{KCl}$ eutectic phase and glass fiber. In addition, it can also be seen that the KCl primary phase displays bulk crystals, which presents white in the backscattered SEM image.

Figure 6 exhibits SEM morphologies of the KNO_3 -based salt cores strengthened by different sizes and contents glass fibers. It can be observed from Figure 6a that the unreinforced KNO_3 -based salt core possesses coarse dendrites. However, the microstructures are dramatically refined and improved when the KNO_3 -based salt core is strengthened by the glass fiber. As shown in Figure 6b–d, the size of the glass fiber is 75 μm , and the contents of the glass fiber are 10 wt.%, 20 wt.% and 30 wt.%, respectively. It is clear that the size of the KCl primary phase decreases with the increase in the glass fiber content, and the glass fibers are distributed around the KCl primary phase. Meanwhile, the

coarse dendrites gradually become bulk or petal-like crystals, and many fiber pull-out holes are observed. As shown in Figure 6e–g, the size of the glass fiber is 25 μm , as the glass fiber content increases from 10 wt.% to 30 wt.%, the size of the KCl primary phase shows a similar trend compared to 75- μm glass fiber, and the KCl primary phase is homogeneously distributed in the salt core. As shown in Figure 6h–j, the size of the glass fiber is 12.5 μm , many short glass fibers are embedded in the salt core, and the finer KCl primary phase is observed.

Table 3 shows the quantitative analysis results for the microstructure of the KNO_3 -based salt core strengthened by different sizes and contents glass fibers. The quantitative analysis including the average grain size of the KCl primary phase and the number of fiber pull-out holes is calculated according to Figure 6. As can be seen from Table 3, the glass fiber significantly reduces the grain size of the KCl primary phase compared with the unreinforced condition. For the unreinforced KNO_3 -based salt core, the average grain size of the KCl primary phase is $58.98 \pm 5.54 \mu\text{m}$, and the number of the fiber pull-out holes is 0. For the KNO_3 -based salt core strengthened by the glass fiber. When the glass fiber size is 74 μm , with the increase in the glass fiber content from 10 wt.% to 30 wt.%, the average grain size of the KCl primary phase reduces from $40.07 \pm 4.30 \mu\text{m}$ to $23.63 \pm 2.15 \mu\text{m}$. When the glass fiber size is 12.5 μm , with the increase in the glass fiber content from 10 wt.% to 30 wt.%, the average grain size of the KCl primary phase reduces from $22.39 \pm 2.13 \mu\text{m}$ to $11.97 \pm 1.27 \mu\text{m}$. Meanwhile, when the glass fiber content is 30 wt.%, with the decrease in the glass fiber size from 74 μm to 12.5 μm , the average grain size of the KCl primary phase reduces from $23.63 \pm 2.15 \mu\text{m}$ to $11.97 \pm 1.27 \mu\text{m}$. This grain refinement of the KCl primary phase is mainly attributed to two factors. On the one hand, the skeleton structure formed by glass fibers in the KNO_3 -based salt core matrix limits the growth of grains. On the other hand, the glass fiber as a foreign medium promotes the heterogeneous nucleation of the KCl primary phase. Moreover, the larger size and content of the glass fiber make more fiber pull-out holes. Therein, when the glass fiber size is 74 μm , with the

increase in the glass fiber content from 10 wt.% to 30 wt.%, the number of the fiber pull-out holes increases from 5 to 15. when the glass fiber size is 12.5 μm , the number of the fiber pull-out holes is 0 or 1. It is well known that the grain refinement can significantly enhance the strength of materials, and the fiber pull-out is one of the main theories that explains the improvement in the toughness.^{27,28} This result is in good agreement with previous studies shown in Figure 3.

Figure 7 depicts the SEM images of crack propagation in the KNO_3 -based salt core strengthened by 12.5- μm glass fiber. It is well known that the toughening mechanism of the glass fiber includes fiber pull-out, crack bridging and crack deflection, among which the fiber pull-out is usually accompanied by the crack bridging.^{29,30} The crack deflection and the crack bridging are founded during the crack propagation, as shown in Figure 7a, c. Meanwhile, the fiber

Figure 6. SEM morphologies of the KNO_3 -based salt cores: (a) unreinforced; (b–d) 75- μm glass fiber with different contents (10 wt.%, 20 wt.%, 30 wt.%); (e–g) 25- μm glass fiber with different contents (10 wt.%, 20 wt.%, 30 wt.%); (h–j) 12.5- μm glass fiber with different contents (10 wt.%, 20 wt.%, 30 wt.%)

pull-out is also observed, as shown in Figure 7b. It can be noted that the glass fiber bridges the crack, preventing the crack propagation, resulting in the improvement in the toughness of the KNO_3 -based salt core, and the schematic diagram of the crack bridging is shown in Figure 7d. As the load is transmitted from the KNO_3 -based salt core matrix to the glass fiber, the glass fiber is pulled out of the matrix when the shear stress generated at the interface reaches the interface shear strength. The fiber pull-out during the crack propagation can cause the energy dissipation, thereby

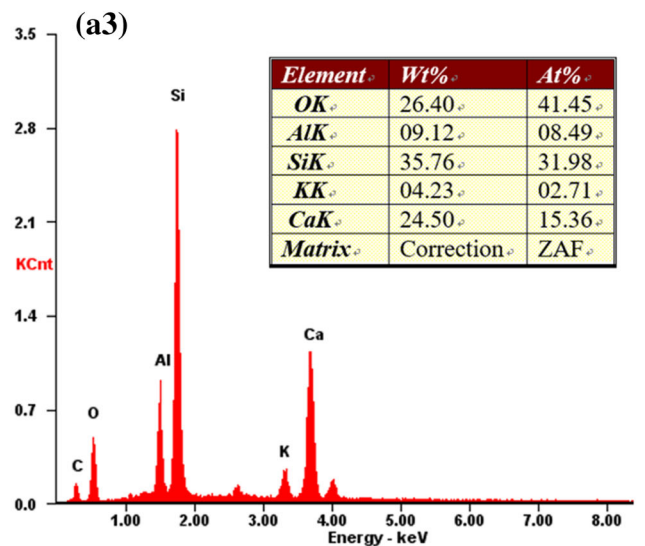
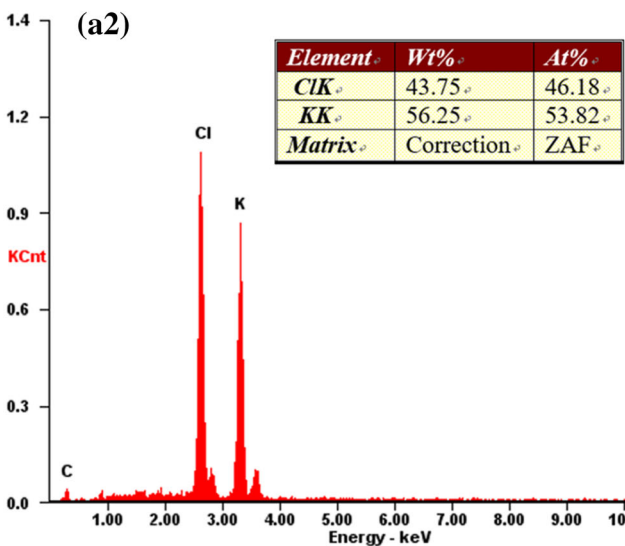
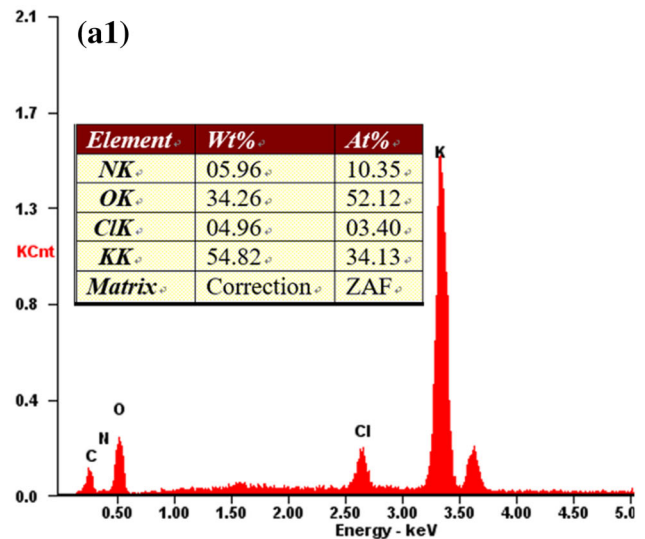
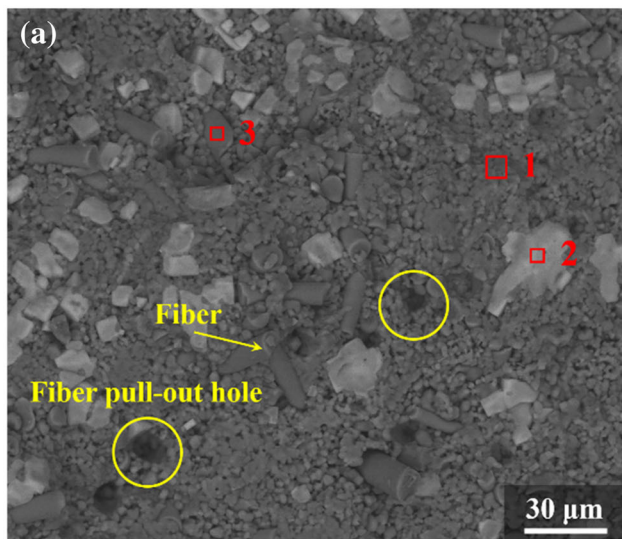


Figure 5. Fracture surface and EDS results of the KNO_3 -based salt core strengthened by 20 wt.% glass fiber (size = 25 μm): (a) Backscattered SEM image and (a1–a3) EDS results labeled in (a)

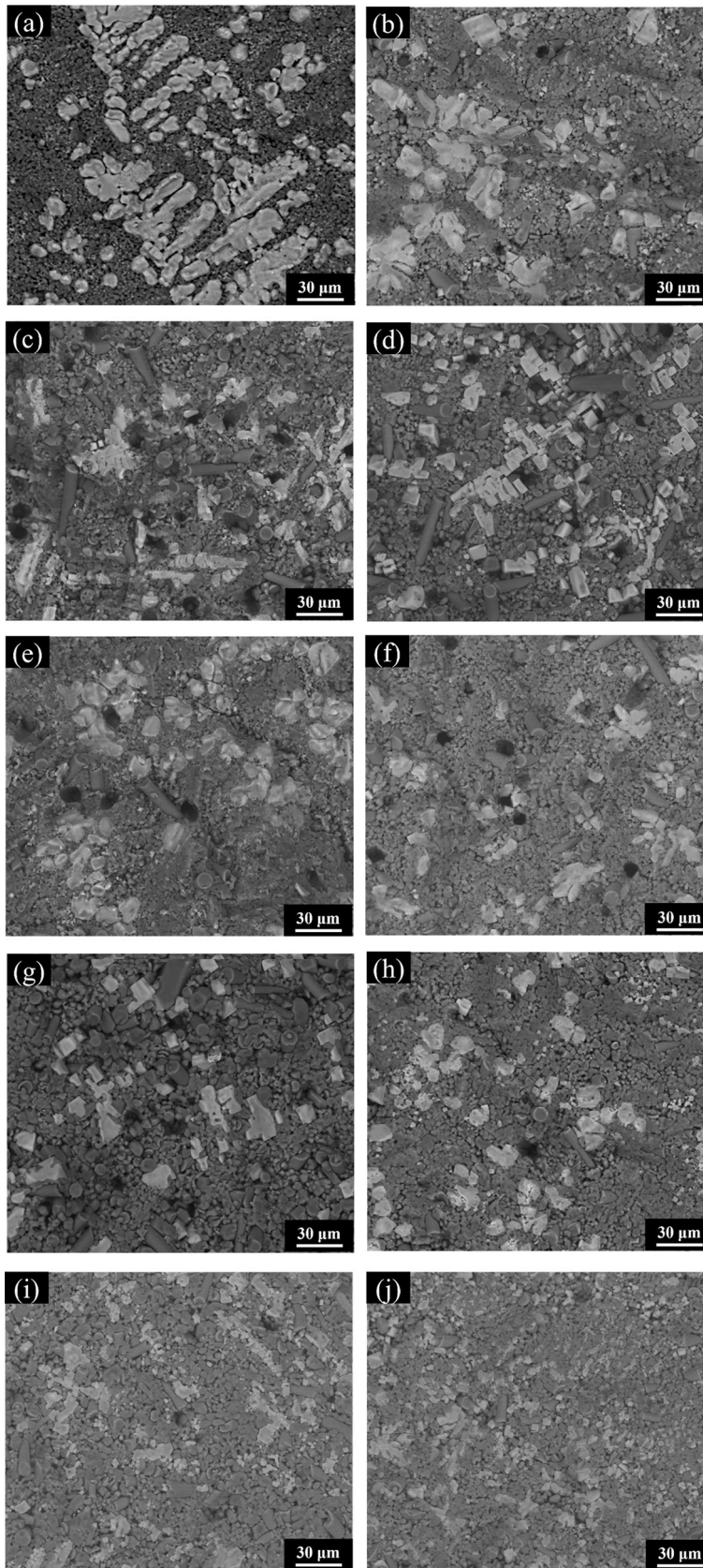


Table 3. Quantitative Analysis Results for the Microstructure of the KNO_3 -Based Salt Core

Glass fiber		Grain size of the KCl primary phase (μm)	Number of fiber pull-out holes
Size (μm)	Content (wt.%)		
–	0 (unreinforced)	58.98 ± 5.54	0
74	10	40.07 ± 4.30	5
	20	29.59 ± 3.84	14
	30	23.63 ± 2.15	15
25	10	30.85 ± 3.91	4
	20	22.24 ± 2.01	8
	30	18.02 ± 1.82	7
12.5	10	22.39 ± 2.13	1
	20	16.62 ± 1.45	1
	30	11.97 ± 1.27	0

enhancing the toughness of the KNO_3 -based salt core, and the schematic diagram of the fiber pull-out is shown in Figure 7e. Moreover, it can be evidently seen from Figure 7c, f that the crack deflection changes the path of the crack propagation, causing more fracture energy to be absorbed, resulting in an improvement in mechanical properties of the KNO_3 -based salt core. On the other hand, as the glass fiber size increases, the path of the crack deflection increases, which consumes more fracture energy.

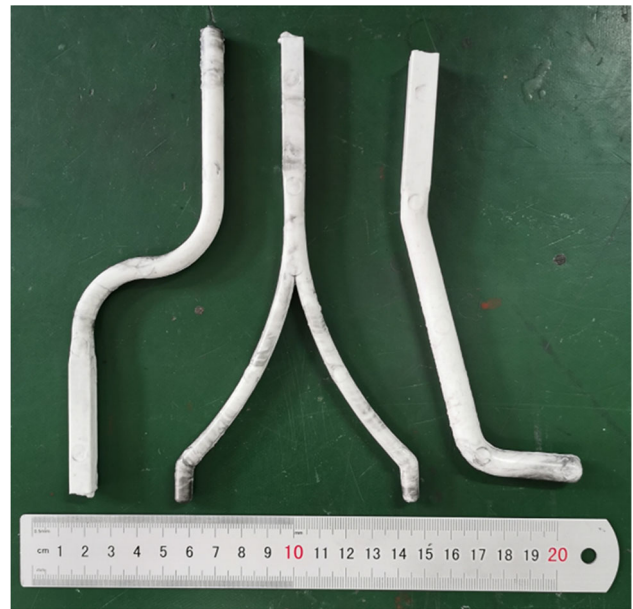


Figure 8. Photographs of complex KNO_3 -based water-soluble salt core strengthened by 30 wt.% glass fiber with 25 μm size

Figure 8 shows a photograph of a complex KNO_3 -based water-soluble salt core strengthened by 30 wt.% glass fiber with 25 μm size. During the process of casting and demolding, the complex salt core did not yield deformation and fracture. As can be seen from Figure 8, the minimum diameter of the complex salt core is about 5 mm, and no defects are found on the surface of the salt core. Meanwhile, the surface roughness of the salt core is 1.9 μm ,

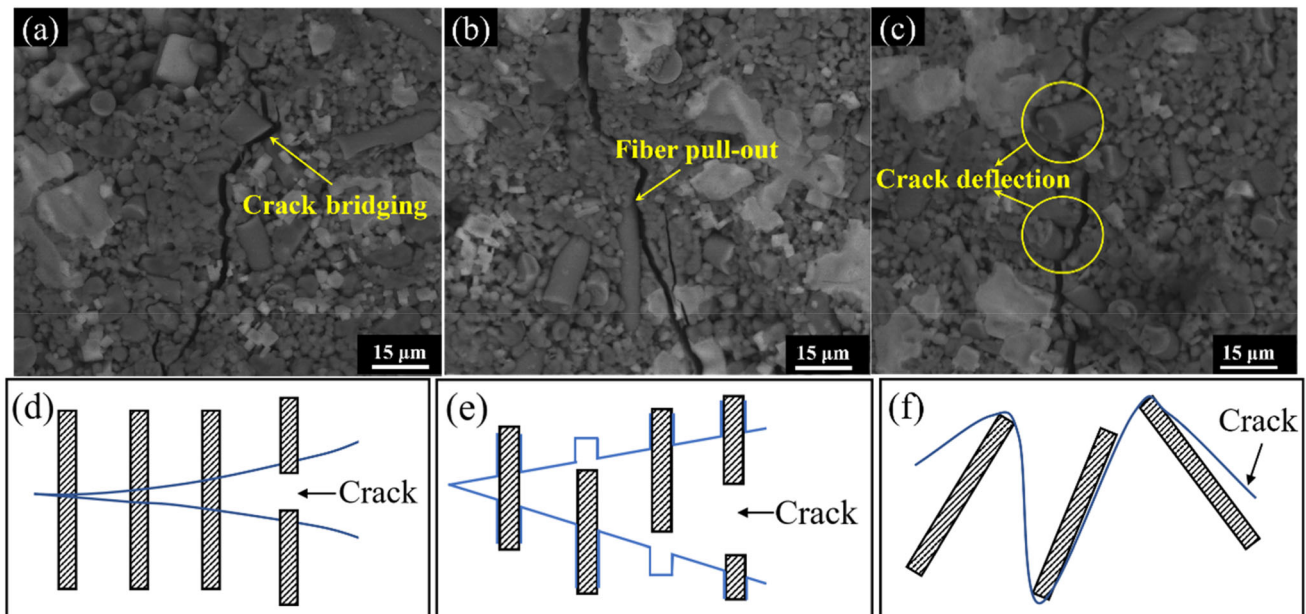


Figure 7. SEM images of crack propagation in the KNO_3 -based salt core strengthened by 12.5- μm glass fiber: (a) 30 wt.% glass fiber; (b) and (c) 20 wt.% glass fiber; (d) the scheme diagram of crack bridging; (e) the scheme diagram of fiber pull-out; and (f) the scheme diagram of crack deflection

which can be used in the production of complex precision parts.³¹

Conclusions

In this study, the effects of glass fiber size and content on the bending strength, impact toughness, water solubility rate, hygroscopic rate and microstructure characteristics of the KNO₃-based water-soluble salt core were investigated. The experimental results were summarized as follows:

1. The size and content of the glass fiber had a remarkable effect on the properties of the KNO₃-based salt core. The bending strength and impact toughness of the KNO₃-based salt core greatly enhanced with the increase in glass fiber content, and increasing the glass fiber size sharply enhanced the impact toughness, while decreased the bending strength. The addition of glass fiber reduced the water solubility rate and hygroscopic rate of the salt core.
2. The glass fiber significantly improved the morphology of the KNO₃-based salt core. Compared with the unreinforced KNO₃-based salt core, the grain size of the KCl primary phase was greatly reduced, and the glass fiber with a small size was more obvious for the KCl primary phase grain refinement. For the glass fiber with a large size, many fiber pull-out holes were observed in the fracture surface of the salt core.
3. The solidification microstructures of the KNO₃-based salt core strengthened by glass fiber were comprised of the KCl primary phase, the KNO₃ + KCl eutectic phase and the glass fiber phase. The glass fibers were evenly distributed in the KNO₃-based salt core, which significantly refined the KCl primary phase, resulting in a remarkable improvement in the bending strength. In addition, the fiber pull-out and crack deflection were the main toughening mechanism for the KNO₃-based salt core.

Acknowledgements

The authors gratefully acknowledge the financial support received from the National Nature Science Foundation of China (No. 51775204), the National MCF Energy R&D Program (No. 2018YFE0313300) and the Research Project of the State Key Laboratory of Materials Processing and Die & Mould Technology and the Analytical and Testing Center, Huazhong University of Science and Technology.

REFERENCES

1. Z. Xiao, L.T. Harper, A.R. Kennedy, N.A. Warrior, A water-soluble core material for manufacturing hollow composite sections. *Compos. Struct.* **182**, 380–390 (2017)
2. R. Huang, B. Zhang, Study on the composition and properties of salt cores for zinc alloy die casting. *Inter Metalcast* **11**, 440–447 (2017). <https://doi.org/10.1007/s40962-016-0086-7>
3. J. Yaokawa, D. Miura, K. Anzai, Y. Yamada, H. Yoshii, Strength of salt core composed of alkali carbonate and alkali chloride mixtures made by casting technique. *Mater. Trans.* **48**, 1034–1041 (2007)
4. Y. Yamada, J. Yaokawa, H. Yoshii, K. Anzai, Developments and application of expendable salt core materials for high-pressure die casting to apply closed-deck type cylinder block, in *JSAE-Report (Society of Automotive Engineers of Japan)*, pp. 1–5 (2007)
5. R.J. Donahue, M.T. Degler, Congruent melting salt alloys for use as salt cores in high pressure die casting: U.S. Patent 9878367 (2018)
6. K. Oikawa, K. Sakakibara, Y. Yamada, High-Temperature Mechanical Properties of NaCl–Na₂CO₃ Salt-Mixture Removable Cores for Aluminum Die-Casting. *Mater. Trans.* **60**, 19–24 (2019)
7. S. Tu, F. Liu, G. Li, W. Jiang, X. Liu, Fabrication and characterization of high-strength water-soluble composite salt core for zinc alloy die castings. *Int J Adv Manuf Tech* **95**, 505–512 (2018)
8. D. Cica, D. Kramar, Intelligent process modeling and optimization of porosity formation in high-pressure die casting. *Int. Metalcast.* **12**, 814–824 (2018). <https://doi.org/10.1007/s40962-018-0213-8>
9. B. Fuchs, H. Eibisch, C. Körner, Core viability simulation for salt core technology in high-pressure die casting. *Int. Metalcast.* **7**, 39–45 (2013). <https://doi.org/10.1007/BF03355557>
10. X.X. Dong, H.L. Yang, X.Z. Zhu, High strength and ductility aluminium alloy processed by high pressure die casting. *J. Alloy. Compd.* **773**, 86–96 (2019)
11. D.E. Grebe, M.P. Potratz, Disintegrative core for use in die casting of metallic components: U.S. Patent 7013948 (2006)
12. Z. Long, Effect of kaolin on tensile strength and humidity resistance of a water-soluble potassium carbonate sand core. *China Foundry* **13**, 15–21 (2016)
13. Y. Youji, Method of manufacturing expendable salt core for casting. U.S. Patent 8574476B (2013)
14. Y.J. Hori, N. Miura, Y. Kurokawa, Water-soluble casting mold and method for manufacturing the same: U.S. Patent 20040238157A1 (2004)
15. K. Hirokawa, Disintegrative core for high pressure casting, method for manufacturing the same, and method for extracting the same: U.S. Patent 6755238 (2004)

16. A. Elsayed, C. Ravindran, B.S. Murty, Effect of aluminum-titanium-boron based grain refiners on AZ91E magnesium alloy grain size and microstructure. *Inter Metalcast* **5**, 29–41 (2011)
17. M. Uludağ, R. Çetin, D. Dispınar, M. Tiryakiođlu, Effect of degassing and grain refinement on hot tearing tendency in Al8Si3Cu alloy. *Inter Metalcast* **12**, 589–595 (2018). <https://doi.org/10.1007/s40962-017-0197-9>
18. P. Jelínek, F. Mikšovský, J. Beňo, E. Adámková, Development of foundry cores based on inorganic salts. *Mater. Tech.* **6**, 689–693 (2013)
19. Z.L. Lu, Y.X. Fan, K. Miao, H. Jing, D.C. Li, Effects of adding aluminum oxide or zirconium oxide fibers on ceramic molds for casting hollow turbine blades. *Int. J. Adv. Manuf. Technol.* **72**, 873–880 (2014)
20. X.W. Yin, Fibre-reinforced multifunctional SiC matrix composite materials. *Int. Mater. Rev.* **62**, 117–172 (2017)
21. K. Lü, X. Liu, Z. Duan, Effect of firing temperature and time on hybrid fiber-reinforced shell for investment casting. *Inter Metalcast* **13**, 666–673 (2019). <https://doi.org/10.1007/s40962-018-0280-x>
22. T.Q. Gao, Fabrication and characterization of three dimensional woven carbon fiber/silica ceramic matrix composites. *Compos Part B-Eng* **77**, 122–128 (2015)
23. L. Wan, P.C. Xu, J.R. Luo, Properties and forming characters of water soluble salt-core reinforced by ceramic whiskers. *Foundry* **57**, 234–238 (2008). (in Chinese)
24. W.M. Jiang, Z.T. Fan, D.F. Liao, Investigation of microstructures and mechanical properties of A356 aluminum alloy produced by expendable pattern shell casting process with vacuum and low pressure. *Mater. Des.* **32**, 926–934 (2011)
25. J.A. Dean, J. Dean, *Analytical chemistry handbook* (McGraw-Hill, New York, 1995)
26. http://www.crct.polymtl.ca/fact/phase_diagram.php?file=KCl-KNO3.jpg&dir=FTsalt
27. W. Yuan, S.K. Panigrahi, J. Su, R.S. Mishra, Influence of grain size and texture on Hall–Petch relationship for a magnesium alloy. *Scripta Mater.* **65**, 994–997 (2011)
28. B. Yu, C. Geng, M. Zhou, Impact toughness of polypropylene/glass fiber composites: interplay between intrinsic toughening and extrinsic toughening. *Compos Part B-Eng* **92**, 413–419 (2016)
29. J.J. Sha, J. Li, S.H. Wang, Toughening effect of short carbon fibers in the ZrB₂-ZrSi₂ ceramic composites. *Mater Design* **75**, 160–165 (2015)
30. J. Njuguna, Z. Mouti, K. Westwood, Toughening mechanisms for glass fiber-reinforced polyamide composites, in *Toughening Mechanisms in Composite Materials*. Woodhead Publishing, pp. 211–232 (2015)
31. S. Tang, L. Yang, G. Li, Effect of the addition of silica sol on layered extrusion forming of Al₂O₃-based cores. *Adv. Appl. Ceram.* **118**, 1–8 (2018)

Publisher's Note Springer Nature remains neutral with regard to jurisdictional claims in published maps and institutional affiliations.